Begell House, Inc. Publishers

Journal Production
50 North Street
Danbury, CT 06810
Phone: 1-203-456-6161
Fax: 1-203-456-6167
Begell House Production Contact : journals@begellhouse.com

Dear Corresponding Author,

Attached is the corresponding author pdf file of your article that has been published.

Please note that the pdf file provided is for your own personal use and is not to be posted on any websites or distributed in any manner (electronic or print). Please follow all guidelines provided in the copyright agreement that was signed and included with your original manuscript files.

Any questions or concerns pertaining to this matter should be addressed to journals@begellhouse.com

Thank you for your contribution to our journal and we look forward to working with you again in the future.

Sincerely,
Michelle Amoroso
Michelle Amoroso
Production Department

Special Topics & Reviews in Porous Media — An International Journal, 6 (4): 353–365 (2015)

MHD NATURAL CONVECTION IN A POROUS EQUILATERAL TRIANGULAR ENCLOSURE WITH A HEATED SQUARE BODY IN THE PRESENCE OF HEAT GENERATION

Raju Chowdhury,[1,2] Salma Parvin,[2] Md. Abdul Hakim Khan,[2] & Ali J. Chamkha[3,*]

[1]*Department of Natural Science, Stamford University Bangladesh, Dhaka-1217, Bangladesh*

[2]*Department of Mathematics, Bangladesh University of Engineering & Technology, Dhaka-1000, Bangladesh*

[3]*Mechanical Engineering Department, Prince Mohammad Bin Fahd University, Al-Khobar 31952, Kingdom of Saudi Arabia*

[*]Address all correspondence to: Ali J. Chamkha, E-mail: achamkha@pmu.edu.sa

Original Manuscript Submitted: 2/23/2015; Final Draft Received: 1/21/2016

The present numerical work is performed to analyze the heat transfer and fluid flow due to free convection in a porous equilateral triangular enclosure with a heated square body in the presence of magnetic field and heat generation. The left inclined wall of the enclosure is adiabatic while the horizontal wall is heated at a uniform temperature; the lower portion of the right inclined wall is considered to be nonisothermal and the upper portion of the wall is cold. The square body is maintained at a constant temperature. The governing equations are solved numerically subject to appropriate boundary conditions by the finite element method using Galerkin's weighted residuals scheme. Results are presented by streamlines, isotherms, mean Nusselt numbers for the different parameters such as Hartmann number (Ha), heat generation (λ), and size of the square body (l_b). The Prandtl number (Pr) and Rayleigh number (Ra) are considered fixed. It is observed that the size of the body plays an important role with regard to the heat and fluid flow inside the cavity.

KEY WORDS: *free convection, MHD, heat generation, equilateral triangular cavity, heated square body, porous media*

1. INTRODUCTION

Natural convection in porous media can be found in many applications of engineering, such as building insulation, grain storage, geothermal problems, geophysical problems, and solar collectors. These applications are well described by Nield and Bejan (2006) and Ingham and Pop (2005).

The phenomena of natural convection in porous enclosures can be classified into two geometrical classes as rectangular and nonrectangular enclosures. Rectangular-shaped cavities (Ostrach, 1972; Hossain and Wilson, 2002; Khanafer and Chamkha, 1998) in porous media have been chosen by most researchers due to simplicity of solutions and practical importance. Some researchers have investigated nonrectangular-shaped enclosures such as triangular (Asan and Namli, 2000; Akinsete and Coleman, 1982; Chamkha and Ismael, 2013; Chamkha and Ismael, 2013a; Chamkha et al., 2010; Chowdhury et al., 2015; Parvin and Hossain, 2012; Varol et al., 2006b), trapezoidal (Baytas and Pop, 1999), and wavy shapes (Varol and Oztop, 2006; Nasrin et al., 2012; Parvin et al.,

NOMENCLATURE

B_0	applied magnetic field strength (T)
C_p	specific heat at constant pressure (J kg^{-1}K^{-1})
Da	Darcy parameter
g	gravitational acceleration (m s^{-2})
Ha	Hartmann number
K	permeability of the porous media (m^2)
k	thermal conductivity of the media (W m^{-1} K^{-1})
L	height of the triangle (m)
l	length of the inclined wall (m)
Nu	Nusselt number
Pr	Prandtl number
p	fluid pressure (Pa)
Ra	Rayleigh number
T	temperature (°C)
t	time (s)
U, V	dimensionless velocity components
u, v	velocity in x, y direction (m s^{-1})
U_0	reference velocity, α/L
X, Y	dimensionless coordinates
x, y	Cartesian coordinates (m)

Greek Symbols

α	thermal diffusivity (m^{2}s^{-1})
β	thermal expansion coefficient of fluid (K^{-1})
γ	fluid ratio of specific heat
ε	porosity
θ	dimensionless temperature
l	dimensionless length
λ	dimensionless heat generation parameter
μ	dynamic viscosity (Pa s^{-1})
υ	kinematic viscosity, μ/ρ (m^2 s^{-1})
ρ	fluid density (kg m^{-3})
σ	electrical conductivity of the fluid (S m^{-1})
τ	dimensionless time

Subscripts

b	square body
c	cold
h	hot

2011). In these studies they have shown that both flow and temperature fields are affected by the geometrical parameters.

The triangular cavities approach with differentially heated isothermal walls has received considerable attention because of its wide applications for roof building, design of industrial equipment, cooling of electronic devices, thermal storage systems, and furnaces, fire control in buildings, and some solar applications.

A few recent studies on natural convection in triangular enclosures have also been carried out for various applications. Varol et al. (2006a), Ridouane et al. (2006), and Joudi et al. (2004) numerically studied the performance of a prism-shaped solar collector with a right-angled triangular cross-sectional area. The effect of horizontal adiabatic partitioning was studied. Tzeng et al. (2005) carried out numerical simulation and parametric studies for triangular enclosures. The aim of this study was to establish efficient energy management.

The characteristics of heat and fluid flow for a configuration of isothermal vertical walls maintained at different temperatures and with adiabatic horizontal walls are well understood Ostrach (1972). The problem of natural convection heat transfer in a triangular enclosure filled with a porous medium was first considered by Bejan and Poulikakos (1982). They found that the porous media can be a control element for heat transfer and fluid flow. Varol et al. (2006b) have studied natural convection in a right angle triangular enclosure filled with a porous medium by taking into account all possibilities of thermal boundary conditions. More recently, Basak et al. (2008) have made a numerical analysis using the finite element method to investigate the effects of nonisothermal boundary conditions on flow fields and temperature distribution in a triangular enclosure filled with a porous medium.

Many authors have recently analyzed heat transfer in enclosures with partitions, fins, and blocks, which manipulates the convective flow phenomenon. A body can be used as a control element for heat transfer and fluid flow, which was investigated by Varol et al. (2007). Amine et al. (2004) investigated thermal convection around obstacles with different configurations. Ha et al. (1999) examined the heat-generating conducting body inserted enclosure. Similarly, Ha et al. (2002) tested the different boundary conditions for the inserted body to the enclosure. They reported that the presence of the body obstructs the flow and temperature fields. Oztop et al. (2001) analyzed the effects of the location of the insulated body for a partially heated enclosure. Chowdhury et al. (2015a) investigated natural convection in a porous triangular enclosure with a circular obstacle in the presence of heat generation.

The buoyancy-driven convection in a rectangular enclosure with a transverse magnetic field was studied by Garandet et al. (1992). The geometry considered in the numerical study of Oh et al. (1997) was that the conducting body generated heat within the cavity. Under these situations, the flow was driven by a temperature difference across the cavity and a temperature difference caused by the heat-generating source.

The effect of the magnetic field on the convective heat transfer and the free convection flow of the fluid are of vital importance in engineering. Several numerical and experimental methods have been developed to investigate flow characteristics inside cavities because these geometries have practical engineering and industrial applications, such as in the design of solar collectors, the thermal design of buildings, air conditioning, and cooling of electronic devices and furnaces. Oztop et al. (2009) numerically investigated the magnetic field effects on natural convection in an enclosure with a nonisothermal heater. The problem of hydromagnetic convection with heat generation or absorption was studied by Chamkha (2002).

According to the knowledge of the authors and the literature given above, there is no study on natural convection heat transfer in an equilateral triangular enclosure containing a heated square body and with both magnetohydrodynamic (MHD) effects and heat generation. The main purpose of this study is to investigate the effect of size of the square body and MHD on free convection heat transfer in a porous-medium-filled equilateral triangular enclosure with heat generation. The bottom wall of the enclosure is heated uniformly, the left inclined wall is adiabatic and the right inclined wall is heated differentially. The tests were performed for different Hartmann numbers, heat generation parameters, and size of the square body.

2. PHYSICAL FORMULATION

The treated problem is an equilateral triangular cavity of height L filled with a fluid-saturated porous medium. The physical system is considered in this study as shown in Fig. 1(a) with the corresponding boundary conditions. The bottom wall is heated isothermally with temperature T_h. The left inclined wall is adiabatic. The upper portion of the right inclined wall is cold and maintained at temperature T_c. The boundary condition at the lower portion of the right inclined wall deserves some explanation: l_1 is the length of a small gap (l is the length of the inclined wall) where the temperature varies linearly from T_h to T_c. A heated square body with length l_b is inserted to the center of the enclosure and is maintained at a uniform temerature T_b such that $T_c < T_b < T_h$. However, gravitational force acts in a vertical direction and a magnetic field of strength B_0 is effective in the horizontal direction normal to the right side wall.

We also bring into account the effect of the temperature-dependent heat-generating flow region. The volumetric heat generation Q is assumed to be

$$Q = \begin{cases} Q_0\,(T - T_c)\,, & T \geq T_c \\ 0, & T \leq T_c \end{cases} \tag{1}$$

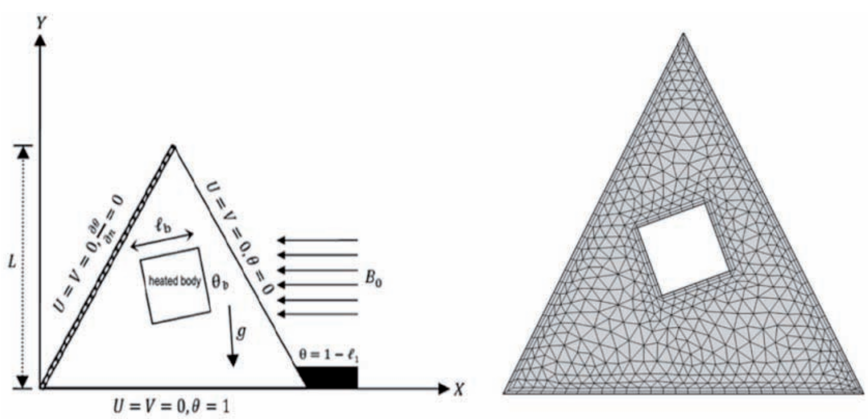

(a) (b)

FIG. 1: (a) Schematic diagram of the enclosure with boundary conditions. **(b)** Mesh structure of elements for triangular enclosure.

where Q_0 is the heat generation constant. The above relation, as explained by Vajravelu and Hadjinicolaou (1997), is valid as an approximation of the state of some exothermic process, which means that heat flows from the surface to the cavity.

3. MATHEMATICAL FORMULATION

In the present problem, we assume unsteady, two-dimensional, laminar flow of a viscous incompressible fluid having constant properties. Under the Boussinesq approximation the dimensionless equations describing the flow are as follows:

$$\frac{\partial U}{\partial X} + \frac{\partial V}{\partial Y} = 0 \tag{2}$$

$$\frac{\partial U}{\partial \tau} + U\frac{\partial U}{\partial X} + V\frac{\partial U}{\partial Y} = -\frac{\partial P}{\partial X} + \mathrm{Pr}\left(\frac{\partial^2 U}{\partial X^2} + \frac{\partial^2 U}{\partial Y^2}\right) - \frac{\mathrm{Pr}}{\mathrm{Da}}U \tag{3}$$

$$\frac{\partial V}{\partial \tau} + U\frac{\partial V}{\partial X} + V\frac{\partial V}{\partial Y} = -\frac{\partial P}{\partial Y} + \mathrm{Pr}\left(\frac{\partial^2 V}{\partial X^2} + \frac{\partial^2 V}{\partial Y^2}\right) - \frac{\mathrm{Pr}}{\mathrm{Da}}V + \mathrm{Ra}\,\mathrm{Pr}\theta - \mathrm{Ha}^2\mathrm{Pr}\,v \tag{4}$$

$$\frac{\partial \theta}{\partial \tau} + U\frac{\partial \theta}{\partial X} + V\frac{\partial \theta}{\partial Y} = \left(\frac{\partial^2 \theta}{\partial X^2} + \frac{\partial^2 \theta}{\partial Y^2}\right) + \lambda\theta \tag{5}$$

where Pr = ν/α is the Prandtl number, Ra = $[g\beta(T_h - T_c)L^3]/(\alpha\nu)$ is the Rayleigh number, Da = $1/\varepsilon = K/L^2$ is the Darcy number, Ha = $B_0 L\sqrt{\sigma/\mu}$ is the Hartmann number, and $\lambda = (Q_0 L^2)/(\rho\nu C_p)$ is the heat generation parameter.

The above equations are nondimensionalized by using the following dimensionless dependent and independent variables:

$$X = \frac{x}{L},\ Y = \frac{y}{L},\ P = \frac{p}{\rho U_0^2},\ l = \frac{l}{L},\ l_1 = \frac{l_1}{L},$$
$$l_b = \frac{l_b}{L},\ \tau = \frac{tU_0}{L},\ U = \frac{u}{U_0},\ V = \frac{v}{U_0},$$
$$\theta = \frac{T - T_c}{T_h - T_c},\ \theta_b = \frac{T_b - T_c}{T_h - T_c} \tag{6}$$

where $U_0 = \alpha/L$ is the reference velocity, X and Y are the coordinates varying along the horizontal and vertical axes, respectively, U and V are the velocity components along the X and Y directions, respectively, θ is the dimensionless temperature, and P is the nondimensional pressure. In the present investigation, the value of the Prandtl number is chosen as 0.7, the Rayleigh number is taken to be 10^5, and the Darcy number is 10^{-3}.

The dimensionless initial and boundary conditions are as follows:

All boundaries are rigid and no-slip: $U = V = 0$ for $\tau = 0$

On the bottom wall: $\theta = 1$

On the left inclined wall: $\partial\theta/\partial n = 0$

On the upper portion of the right inclined wall: $\theta = 0$

On the lower portion of the right inclined wall: $\theta = 1 - l_1$.

At the square body:

For all boundaries: $U = V = 0$; $\theta = \theta_b$, $0 < \theta_b < 1$.

Local and mean Nusselt numbers of the wall are calculated via Eqs. (7) and (8) respectively,

$$\mathrm{Nu} = \frac{hL}{k} = -\frac{\partial\theta}{\partial n}L \tag{7}$$

where h represents the heat transfer coefficient, k thermal conductivity, and n the coordinate direction normal to the surface.

The dimensionless normal temperature gradient can be written as

$$\frac{\partial\theta}{\partial n} = \frac{1}{L}\sqrt{\left(\frac{\partial\theta}{\partial x}\right)^2 + \left(\frac{\partial\theta}{\partial y}\right)^2}$$

and

$$\bar{\mathrm{Nu}} = (1/S)\int_0^s \mathrm{Nu}\,ds \tag{8}$$

where S is the total chord length of the wall and s is the coordinate along the wall.

4. SOLUTION METHODOLOGY

The numerical procedure used in this work is based on the Galerkin weighted residual method of finite element formulation. The application of this technique is well described by Taylor and Hood (1973) and Dechaumphai (1999). In this method, the solution domain is discretized into finite element meshes composed of nonuniform triangular elements. Then the nonlinear governing partial differential equations (i.e., mass, momentum, and energy equations) are transferred into a system of integral equations by applying the Galerkin weighted residual method. The integration involved in each term of these equations is performed by using Gauss's quadrature method. The nonlinear algebraic equations so obtained are modified by imposition of boundary conditions. These modified nonlinear equations are transferred into linear algebraic equations by using Newton's method. Finally, these linear equations are solved by using the triangular factorization method.

5. GRID SENSITIVITY TEST

In the finite element method, the mesh generation is the technique to subdivide a domain into a set of subdomains called finite elements, control volume, etc. The discrete locations are defined by the numerical grid at which the variables are to be calculated. It is basically a discrete representation of the geometric domain on which the problem is to be solved. Mesh generation of elements for the considered cavity is shown in Fig. 1(b). In order to determine the proper grid size for this study, a grid independence test is conducted with four types of mesh for Pr = 0.7, Ra = 10^5, Ha = 0, Da = 10^{-3}, λ = 0 and l_b = 0.2, which are shown in Table 1. The extreme values of average Nusselt number (Nu) are used as the sensitivity measure of the accuracy of the solution and are selected as the monitoring variable. Considering both the accuracy of the numerical values and computational time, the present calculations are performed with a 9055-node and 1087-element grid system.

6. MODEL VALIDATION

The numerical simulation for pure fluid without the MHD effect and a heated square body has been investigated by Saha and Gu (2012) for various values of heat generation parameter with Ra = 10^5 and Pr = 0.7. A test has made to contrast the results obtained by the current model with earlier study Saha and Gu (2012). The results of streamlines and isotherms are given in Figs. 2(a)–2(d) for free convection in a porous triangular cavity. Figures 2(a) and 2(b) present the results of Saha and Gu (2012), and Figs. 2(c) and 2(d) show the results for the present study. The comparison shows that the present results agree with the numerical solution of Saha and Gu (2012). Also, a comparison has been done with Parvin and Nasrin (2011) for MHD free convection in an enclosure containing a heated obstacle with Ra = 10^5, Pr = 0.7 and Ha = 50, and good agreement was found between the present study [Figs. 2(g) and 2(h)] and that of Parvin and Nasrin (2011) [Figs. 2(e) and 2(f)].

TABLE 1: Grid sensitivity check at Pr = 0.7, Ra = $1e^5$, Ha = 0, Da = 10^{-3}, and λ = 0

Nodes	3783	6650	9055	12682
(Elements)	(413)	(760)	(1087)	(1579)
Nu	8.2163	8.2123	8.2111	8.2111
Time (s)	60	85	105	190

7. RESULTS AND DISCUSSION

The hydromagnetic natural convection phenomenon with heat generation effect inside an equilateral triangular obstructed cavity with a heated square obstacle is influenced by different controlling parameters such as Ha, Ra, Pr, λ, Da and the size of the square body l_b. The results are analyzed by obtaining streamlines, isotherms, and average Nusselt number for three parameters varied as $0 \leq \lambda \leq 15$, $0 \leq$ Ha ≤ 60 and $0.1 \leq l_b \leq 0.3$, while the other parameters Pr, Ra and Da are remained fixed at 0.7, 10^5, and 10^{-3}, respectively.

Figure 3 illustrates the effects of the size of the square body with the four different values of heat generation parameter λ on streamlines as well as isotherms while Pr = 0.7, Ra = 10^5, Da = 10^{-3}, and Ha = 0. For the lowest value of λ and l_b [Fig. 3(a)], a triangular-shaped flow distribution is formed. As λ increases from 0 to 15, a vortex is created at the left corner of the square body for fixed l_b. Moreover, the number of vortices present in the primary flow pattern increases due to increasing heat generation. The increase of λ causes acceleration of the fluid motion and enhancement in the maximum temperature. In fact, the increase in the heat generation parameter indicates the increase in heat acquired for the fluid which enhances the natural convection flow. It must be noticed that the size of the vortices increased dramatically for l_b = 0.3. This happened because of the increasing size of the solid body, which gives rise to a decrease in space available for the flow induced by the heat generation. An eddy is created at just above the upper wall of the square body as the heat generation increases. Thus streamlines change apprecibly for both of the previously mentioned parameters.

Figure 4 shows that a heated boundary layer is formed adjacent to the bottom surface as the surface is heated uniformly. As a result of the buoyancy effect, the hot fluid moves uphill from the bottom within the cavity. As the square body is heated, a vortex is created around the body with the increase of heat generation. The higher flow strength can be shown at the right inclined wall of the cavity when l_b = 0.1 and l_b = 0.2. This happens due to high temperature differences between the hot and cold fluid.

The effects of l_b and Hartmann number Ha on streamlines are represented in Fig. 5 while Pr = 0.7, Ra = 10^5,

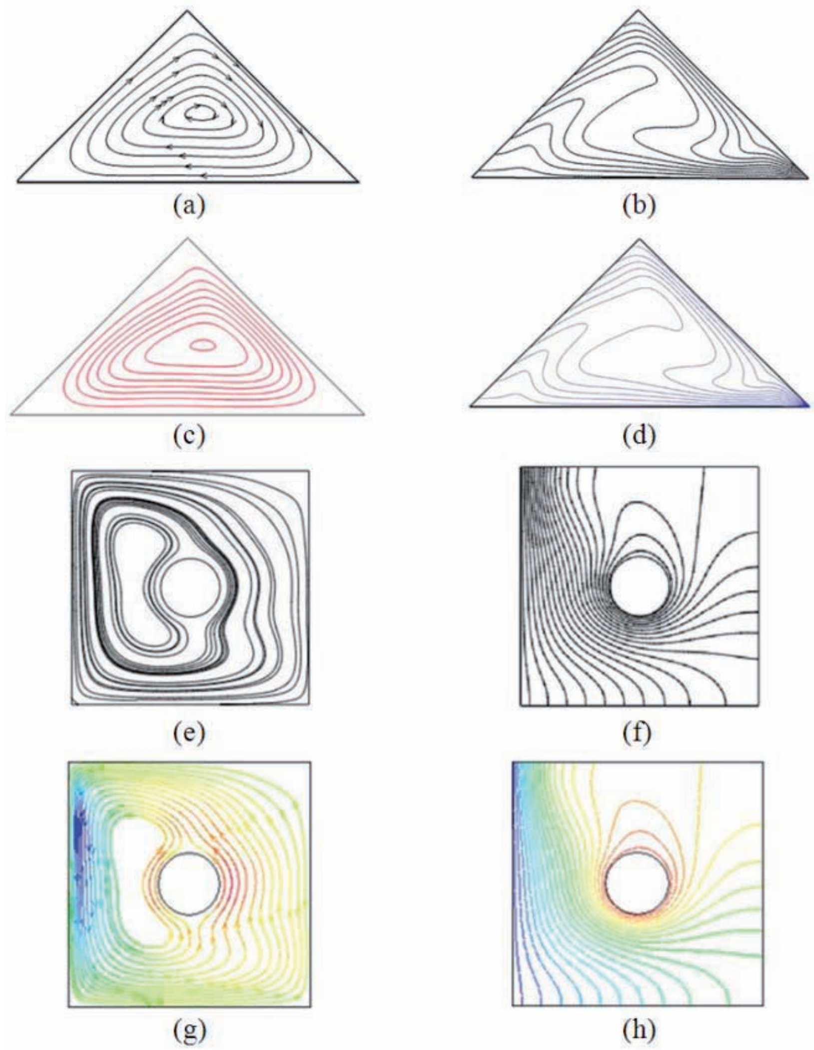

FIG. 2: A comparison for streamlines (left column) and isotherms (right column) with Saha and Gu (2012) **(a, b)** and present study **(c, d)** for Ra = 10^5, Pr = 0.7, Da = 10^{-3}, λ = 0 and Ha = 0 and Parvin and Nasrin (2011) **(e, f)** and present study **(g, h)** for Ra = 10^5, Pr = 0.7 and Ha = 50.

Da = 10^{-3}, and λ = 0. The flow field modifications for all values of Ha are due to variation of l_b. In Fig. 5(a), the flow structure in the absence of magnetic field (Ha = 0) is exposed. The flow with Ha = 0 and l_b = 0.3 produces two eddies just at the bottom part of the square obstacle. The eddy moves at the right corner of the cavity with a mounting magnetic parameter. This is because the applied transverse magnetic field retards the fluid motion. For l_b = 0.1 and l_b = 0.2, a vortex is created at the bottom of the square body. The size of the vortex increases with the increase of Hartmann number.

In Fig. 6, the corresponding isothermal lines are plotted. For Ha = 0, the isothermal lines form a thin thermal boundary layer near the bottom wall of the cavity which are becoming linear and parallel with growing Ha. This occurs because the magnetic field acts in the opposite direction to that of the fluid flow.

The variation of Nu at the heated surface for different Hartmann numbers Ha and heat generation parameter λ along with size parameter l_b is depicted in Figs. 7(a) and 7(b). Here Nu is plotted as a function of l_b. From Fig. 7(a), it is observed that the rate of heat transfer de-

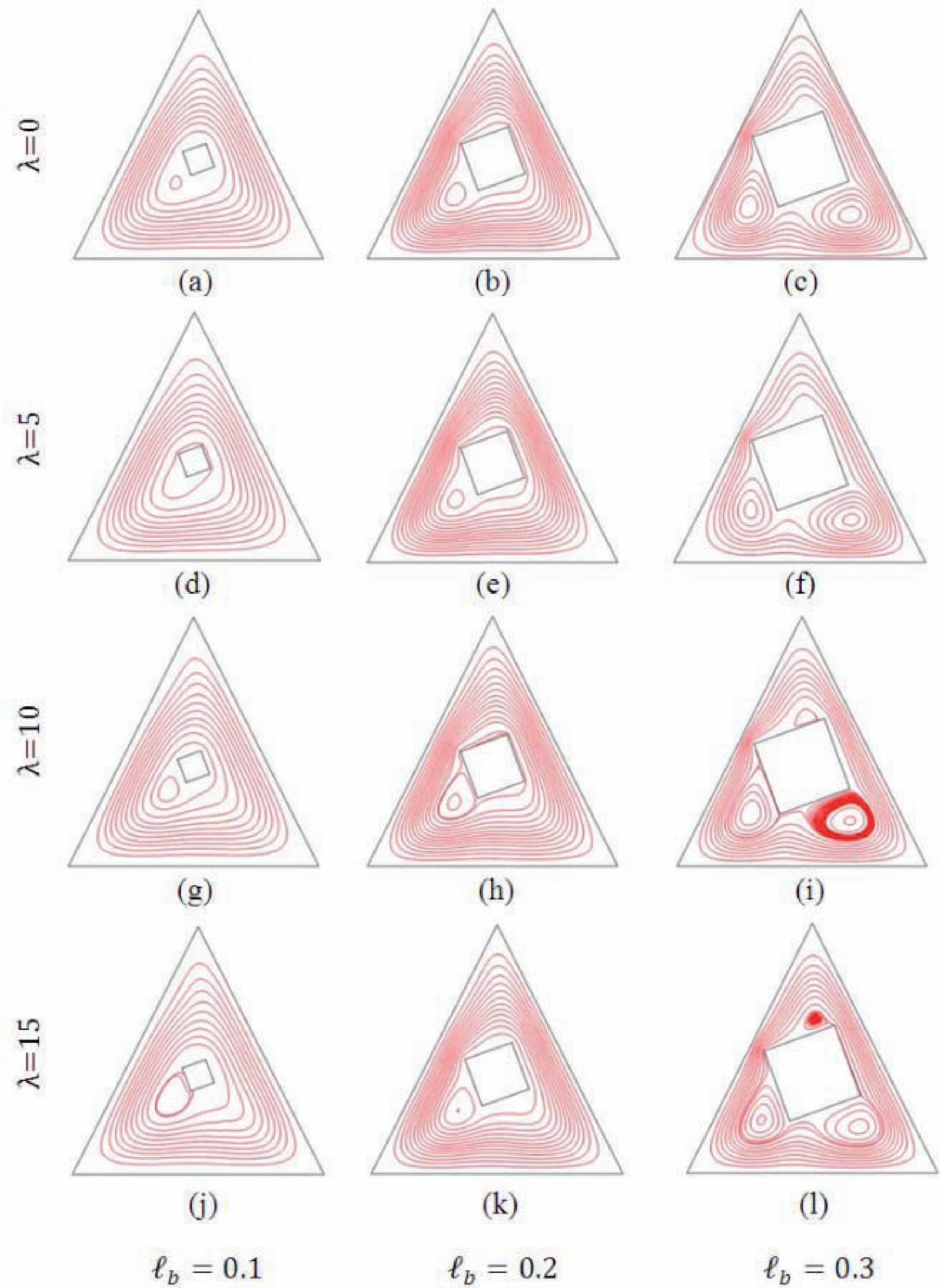

FIG. 3: Streamlines for different sizes of the square cavity l_b and heat generation parameter λ with Ra = 10^5, Pr = 0.7, Da = 10^{-3}, and Ha = 0.

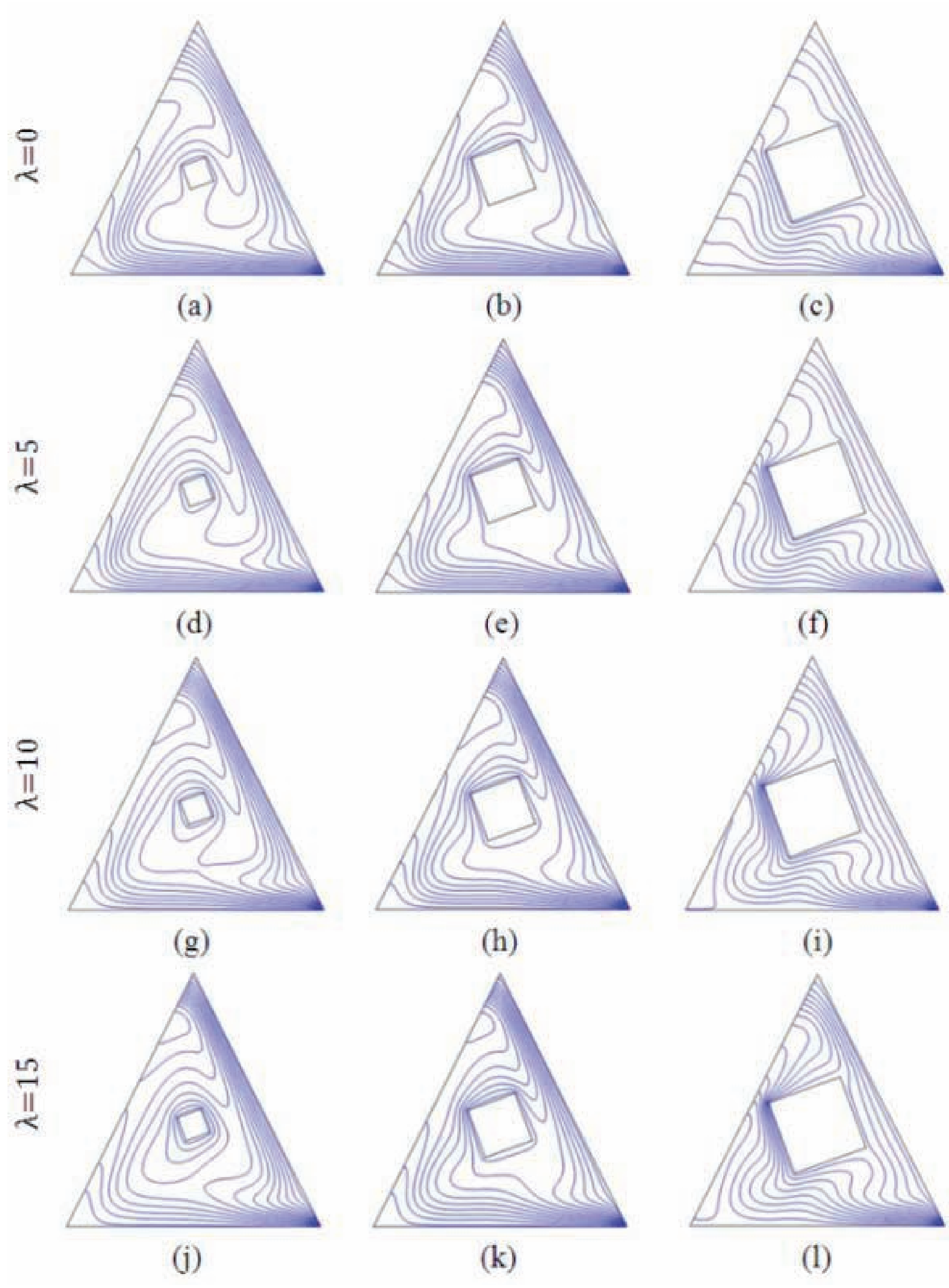

FIG. 4: Isotherms for different sizes of the square cavity l_b and heat generation parameter λ with Ra = 10^5, Pr = 0.7, Da = 10^{-3}, and Ha = 0.

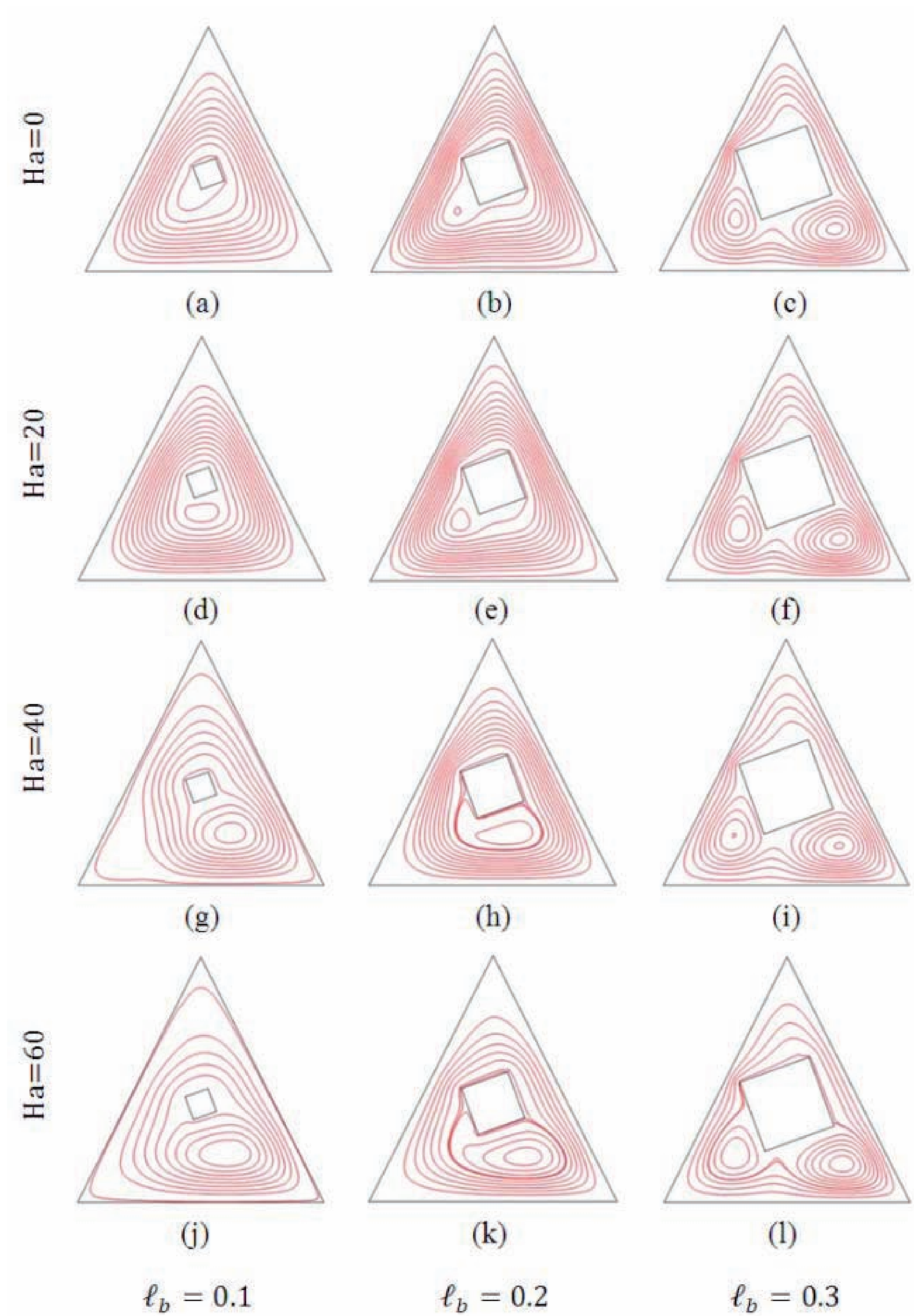

FIG. 5: Streamlines for different sizes of the square cavity l_b and Hartmann number Ha with Ra = 10^5, Pr = 0.7, Da = 10^{-3}, and λ = 0.

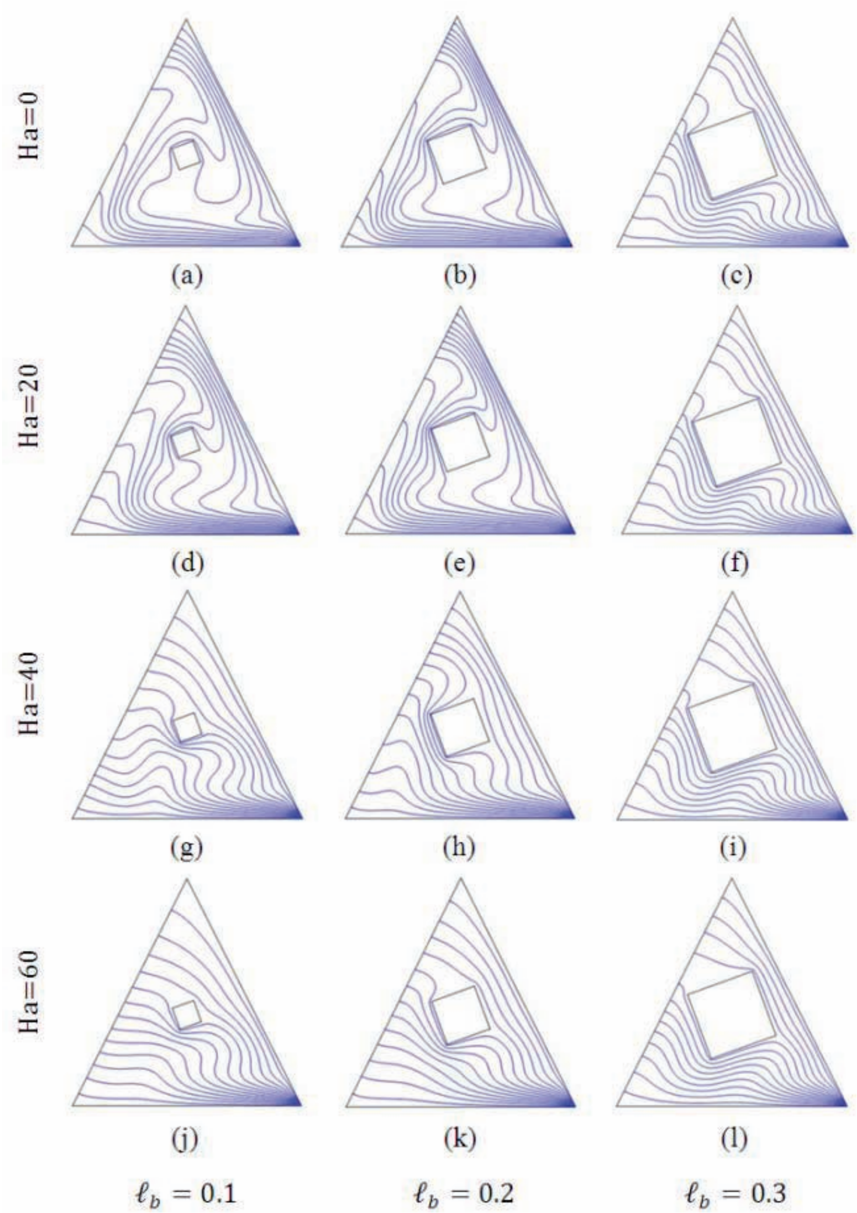

FIG. 6: Isotherms for different sizes of the square cavity l_b and Hartmann number Ha with Ra = 10^5, Pr = 0.7, Da = 10^{-3}, and λ = 0.

creases due to the increase of Ha as the magnetic field acts in the opposite direction of the flow and thus retards the motion. In Fig. 7(b), we see that the rate of heat transfer from the heated bottom surface decreases with the increase in the value of the heat generation parameter. This is expected, since the heat generation mechanism will increase the fluid temperature near the bottom surface, resulting in increased resistance to the transfer of heat in the vertical direction.

8. CONCLUSION

A numerical work is performed to investigate the effect MHD and heat generation on hydromagnetic free convec-

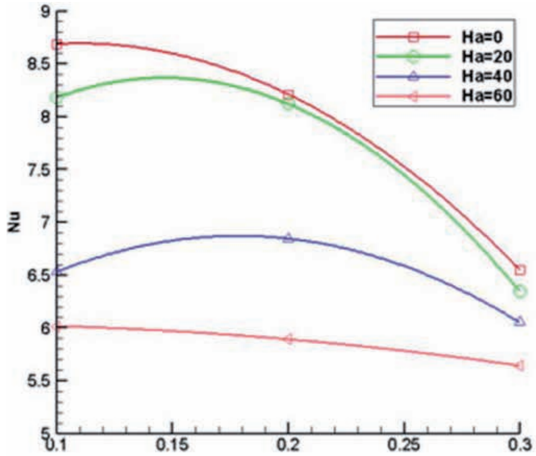

(a)

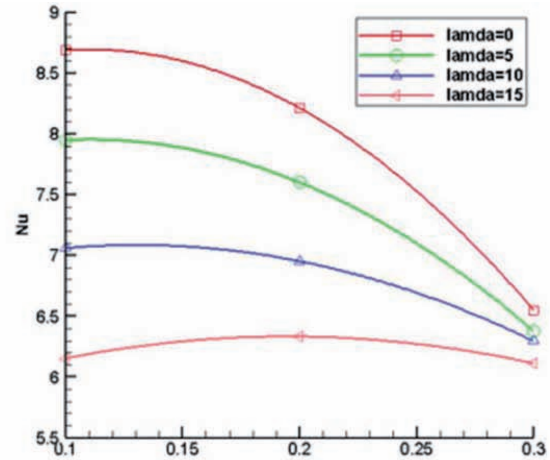

(b)

FIG. 7: Effect of size of the square body l_b on Nu with different values of **(a)** Hartmann number (Ha) and **(b)** heat generation parameter (λ).

tion in a porous equilateral triangular cavity with a heated square obstacle in the presence of heat generation. Some findings can be listed as follows:

- Both heat transfer and fluid flow are affected by the size of the heated square body. Fluid flow is hampered with increasing of size of the body.
- The number of vortices in the streamlines increases with the increase of size of the square body.
- The increase of Hartmann number hinders the flow and consequently, the isothermal lines occupy almost the whole region.
- Fluid flow rate increased with the increase of the heat generation parameter.
- The heat transfer rate at the heated wall was stepped down with the stepping up of the Hartmann number, as well as the heat generation parameter.

ACKNOWLEDGMENTS

This work is supported by the Department of Mathematics, Bangladesh University of Engineering and Technology and Department of Natural Science, Stamford University, Bangladesh.

REFERENCES

Akinsete, V. A. and Coleman, T. A., Heat transfer by steady laminar free convection in triangular enclosures, *Int. J. Heat Mass Transfer*, vol. **25**, pp. 991–998, 1982.

Amine, A., Platten, J. K., and Hasnaoui, M., Thermal convection around obstacles: The case of Sierpinski carpets, *Exp. Fluids*, vol. **36**, pp. 717–727, 2004.

Asan, H. and Namli, L., Laminar natural convection in a pitched roof of triangular cross-section: Summer day boundary conditions, *Energy Build.*, vol. **33**, pp. 69–73, 2000.

Basak, T., Thirumalesha, C., and Roy, S., Finite element simulations of natural convection in a right-angle triangular enclosure filled with a porous medium: Effects of various thermal boundary conditions, *J. Porous Media*, vol. **11**, pp. 159–178, 2008.

Baytas, A. C. and Pop, I., Free convection in oblique enclosures filled with a porous medium, *Int. J. Heat Mass Trans.*, vol. **42**, pp. 1047–1057, 1999.

Bejan, A. and Poulikakos, D., Natural convection in an attic-shaped space filled with porous material, *J. Heat Transfer*, vol. **104**, pp. 241–247, 1982.

Chamkha, A. J., Hydromagnetic combined convection flow in a vertical lid-driven cavity enclosure with internal heat generation or absorption, *Numer. Heat Transfer, Part A*, vol. **41**, pp. 529–546, 2002.

Chamkha, A. J. and Ismael, M. A., Conjugate heat transfer in a porous cavity heated by triangular thick wall, *Numer. Heat Transfer, Part A*, vol. **63**, pp. 144–158, 2013.

Chamkha, A. J. and Ismael, M. A., Conjugate heat transfer in a porous cavity filled with nanofluids and heated by triangular thick wall, *Int. J. Therm. Sci*., vol. **67**, pp. 135–151, 2013a.

Chamkha, A. J., Ismael, M. A., and Ahmad, S. E., Double-diffusive natural convection in inclined finned triangular porous enclosures in the presence of heat generation/absorption effects, *Heat Mass Transfer*, vol. **46**, pp. 757–768, 2010.

Chowdhury, R., Parvin, S., Khan, M. A. H., and Chamkha, A. J., Effect of magnetic field and heat generation on free convection in a porous media filled equilateral triangular cavity, *Int. J. Energy Technol*., vol. **7**, pp. 49–61, 2015.

Chowdhury, R., Khan, M. A. H., and Siddiki, M. N. A., Natural convection in porous triangular enclosure with a circular obstacle in presence of heat generation, *Am. J. Appl. Math*., vol. **3**, pp. 51–58, 2015a.

Dechaumphai, P., *Finite Element Method in Engineering*, 2nd ed., Chulalongkorn University Press, Bangkok, 1999.

Garandet, J. P., Alboussiere, T., and Moreau, R., Buoyancy driven convection in a rectangular enclosure with transverse magnetic field, *Int. J. Heat Mass Transfer*, vol. **35**, pp. 741–748, 1992.

Ha, M. Y., Jung, M. J., and Kim, Y. S., Numerical study on transient heat transfer and fluid flow of natural convection in an enclosure with a heat-generating conducting body, *Numer. Heat Transfer, Part A*, vol. **35**, pp. 415–433, 1999.

Ha, M. Y., Kim, I. K., Yoon, H. S., Yoon, K. S., Lee, J. R., Balachandar, S., and Chun, H. H., Two-dimensional and unsteady natural convection in a horizontal enclosure with a square body, *Numer. Heat Transfer, Part A*, vol. **41**, pp. 183–210, 2002.

Hossain, M. A. and Wilson, M., Natural convection flow in a fluid-saturated porous medium enclosed by non-isothermal walls with heat generation, *Int. J. Therm. Sci*., vol. **41**, pp. 447–454, 2002.

Ingham, D. B. and Pop, I., *Transport Phenomena in Porous Media II*, Pergamon, New York/Los Angeles/Paris/London, 2005.

Joudi, K. A., Hussein, I. A., and Farhan, A. A., Computational model for a prism shaped storage solar collector with a right triangular cross section, *Energy Convers. Manage*., vol. **45**, pp. 391–409, 2004.

Khanafer, K. and Chamkha, A. J., Hydromagnetic natural convection from an inclined porous square enclosure with heat generation, *Numer. Heat Transfer, Part A*, vol. **33**, pp. 891–910, 1998.

Nasrin, R., Parvin, S., Alim, M. A., and Chamkha, A. J., Non-Darcy forced convection through a wavy porous channel using CuO nanofluid, *Int. J. Energy Technol*., vol. **4**, pp. 1–8, 2012.

Nield, D. A. and Bejan, A., *Convection in Porous Media*, 2nd ed., Springer, New York, 2006.

Oh, J. Y., Ha, M. Y., and Kim, K. C., Numerical study of heat transfer and flow of natural convection in an enclosure with a heat generating conducting body, *Numer. Heat Transfer, Part A*, vol. **31**, pp. 289–304, 1997.

Ostrach, S., Natural convection in enclosures, *Adv. Heat Transfer*, vol. **8**, pp. 161–227, 1972.

Oztop, H. F., Dagtekin, I., and Duranay, M., Analysis of natural convection problem in a cavity with partially heated and block inserted, *Proc. of the 13th Heat Science and Technology Congress* (In Turkish), Turkey, pp. 217–222, 2001.

Oztop, H. F., Oztop, M., and Varol, Y., Numerical simulation of magnetohydrodynamic buoyancy-induced flow in a non-isothermally heated square enclosure, *Commun. Nonlinear Sci. Numer. Simul.*, vol. **14**, pp. 770–778, 2009.

Parvin, S. and Nasrin, R., Analysis of the flow and heat transfer characteristics for MHD free convection in an enclosure with a heated obstacle, *Nonlinear Anal. Modell. Control*, vol. **16**, pp. 89–99, 2011.

Parvin, S. and Hossain, N. F., Finite element simulation of MHD combined convection through a triangular wavy channel, *Int. Commun. Heat Mass Transfer*, vol. **39**, pp. 811–817, 2012.

Parvin, S., Alim, M. A., and Hossain, N. F., MHD mixed convection heat transfer through vertical wavy isothermal channels, *Int. J. Energy Technol*., vol. **3**, pp. 1–9, 2011.

Ridouane, E., Campo, A., and Hasnaoui, M., Benefits derivable from connecting the bottom and top walls of attic enclosure with insulated vertical side walls, *Numer. Heat Transfer, Part A*, vol. **49**, pp. 175–193, 2006.

Saha, S. C. and Gu, Y. T., Free convection flow in a triangular enclosure with fluid-saturated porous medium enclosed with heat generation, *J. ANZIAM*, vol. **53**, pp. C127–C141, 2012.

Taylor, C. and Hood, P., A numerical solution of the Navier-Stokes equations using finite element technique I, *Comput. Fluids*, vol. **1**, pp. 73–89, 1973.

Tzeng, S. C., Liou, J. H., and Jou, R. Y., Numerical simulation-aided parametric analysis of natural convection in a roof of triangular enclosures, *Heat Transfer Eng*., vol. **26**, pp. 69–79, 2005.

Vajravelu, K. and Hadjinicolaou, A., Convective heat transfer in an electrically conducting fluid at a stretching surface with uniform free stream, *Int. J. Eng. Sci*., vol. **34**, pp. 1237–1244, 1997.

Varol, Y. and Oztop, H. F., Free convection in a shallow wavy enclosure, *Int. Commun. Heat Mass Transfer*, vol. **33**, pp. 764–771, 2006.

Varol, Y., Koca, A., and Oztop, H. F., Numerical convection in a triangle enclosure with flush mounted heater on the wall, *Int. Commun. Heat Mass Transfer*, vol. **33**, pp. 951–958, 2006a.

Varol, Y., Oztop, H. F., and Varol, A., Free convection in porous media filled right-angle triangular enclosures, *Int. Commun. Heat Mass Transfer*, vol. **33**, pp. 1190–1197, 2006b.

Varol, Y., Oztop, H. F., and Yilmaz, T., Two dimensional natural convection in a porous triangular enclosure with a square body, *Int. Commun. Heat Mass Transfer*, vol. **34**, pp. 238–247, 2007.